Comparison of Catalytic Activities for Sonocatalytic, Photocatalytic and Sonophotocatalytic Degradation of Methylene Blue in the Presence of Magnetic Fe_3O_4/CuO/ZnO Nanocomposites

Ardiansyah Taufik[1,2], Hendry Tju[1,2], and Rosari Saleh[1,2,a]
[1]Departemen Fisika, Fakultas MIPA-Universitas Indonesia, 16424 Depok, Indonesia.
[2]Integrated Laboratory of Energy and Environment, Fakultas MIPA-Universitas Indonesia, 16424 Depok, Indonesia.

[a]Corresponding's author: rosari.saleh@gmail.com ;rosari.saleh@ui.ac.id

Abstract
Fe_3O_4/CuO/ZnO nanocomposites with different molar ratio were synthesized using sol-gel method. The as-synthesized samples were characterized by X-ray diffraction (XRD), UV-visible spectroscopy, BET surface area analyszer, and Electron Spin Resonance (ESR). The sonocatalytic-photocatalytic-sonophotocatalytic activity of as-synthesized samples was investigated based on methylene blue degradation. Moreover, the role of active species was investigated using scavenger technique. The results showed that hole plays an important key role in sono-photo-sonophotocatalytic degradation of methylene blue.

1. Introduction

Methylene blue is widely used in many textile industries. The discharge of methylene blue into wastewater has received a global concern, since it is an environmental hazards. Therefore removal methylene blue from the environment becomes an important issue. Many methods have been investigated for their removal [1-4], however, they are nondestructive methods that only transfer organic pollutant from wastewater to another phase and can easily causing secondary pollution [5].

Sonocatalytic and photocatalytic techniques applied for wastewater treatment have attracted great interest by introducing ultrasonic wave and solar energy without secondary pollution [6-7]. Nanocomposites catalysts by using metal oxide materials have been applied and exhibited some catalytic activity for organic pollutant degradation. It is known that the two most important processes in the degradation of organic pollutants are adsorption and oxidation. Fe_3O_4, a member of the inverse cubic spinel type ferrites, has been found to possess ferromagnetic behavior, and it can be used as an adsorbent. Fe_3O_4, adsorbents engineered with photo- or sonocatalytic ingeredients such as ZnO and CuO can make them multifunctional nanocomposites catalyst [8].

The simultaneous use of sonocatalysis and photocatalysis called sonophotocatalysis has been studied regarding process efficiency to degrade various organics in model solutions [9-14]. The sonophotocatalytic process of oxidation shows interesting advantages at kinetic level, due to the occurance of a synergistic effect between sonolysis and photocatalysis [9-14].

Therefore the aim of this work was to study the degradation of methylene blue by ultrasonic irradiation, UV light irradiations and the combination of ultrasonic as well as UV light irradiations in the presence of Fe_3O_4/CuO/ZnO nanocomposites. The influence of different ZnO loading of Fe_3O_4/CuO/ZnO nanocomposites in the aqueous solution on the sonocatalytic, photocatalytic and sonophotocataltic efficiency was investigated, especially the mechanism taken place at the degradation processes.

2. Experimental details

CuO and Fe_3O_4 nanoparticles and Fe_3O_4/CuO/ZnO nanocomposites were synthesized using a sol-gel method described in our previous study [8]. The samples were characterized by X-ray diffraction (XRD) measurements using a Philips PW 1710 (CuKα = 1.54 Å). UV-Vis diffuse reflectance spectra were measured using a Shimadzu spectrophotometer with an integrating sphere. Magnetic measurements were performed on Oxford Type 1.2T vibrating sample magnetometer (VSM). These measurements were taken from 0 to 1 T. The nitrogen adsorption/desorption isotherms were measured using Nova Quantachrome 2000. The total surface area and pore size distribution were determined via BET and BJH methods. Electron spin resonance (ESR) was performed using X-band JEOL JES-RE1X at room temperature and X-band spectrometer equipped with a 9.1 GHz field modulation unit. Methylene blue (MB) was selected as models of organic pollutants. Sonocatalytic activity was evaluated by degradation of organic pollutants in the presence of Fe_3O_4/CuO/ZnO nanocomposite in aqueous solutions using ultrasonic bath operated at fixed frequency and power of 40 kHz and 150 W, respectively. In photocatalytic measurements, the experimental setup published previously was used [8]. The experimental setup of sonophotocatalytic system composed of ultrasonic bath operated at 40 kHz frequency with 150 W power and 40 W UV lamps. In all experiments, 0.03 g Fe_3O_4/CuO/ZnO nanocomposite was suspended in 100 mL MB solution with a concentration of 20 mg/L. The suspended solution was placed in the dark for 30 min under magnetic stirring to ensure the establishment of an adsorption-desorption equilibrium in MB solution [15]. After that period of time, the ultrasonic bath was turned on and this was taken as “time zero” for the reaction. The samples were collected for 2h at regular intervals. The solution was analyzed using a Dynamica UV-visible spectrophotometer with a quartz cuvette with an optical length of 10 mm.

3. Results and discussion

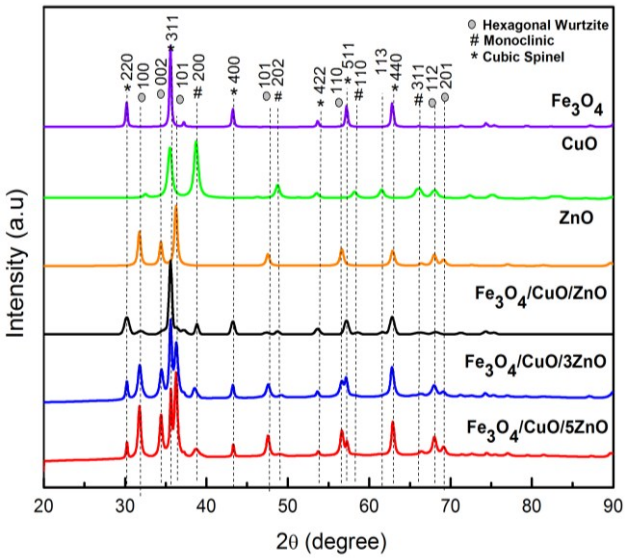

Figure 1. XRD Pattern of pure Fe_3O_4, CuO, ZnO nanoparticle and nanocomposite Fe_3O_4/CuO/ZnO with different molar ratio.

Table 1. Lattice constant and grain size of pure Fe_3O_4, CuO, ZnO nanoparticles and Fe_3O_4/CuO/ZnO nanocomposites with different molar ratio.

Sample	Lattice Parameter (Å)						<D> (nm)		
	ZnO		CuO			Fe_3O_4			
	a=b	c	a	b	c	a=b=c	ZnO	CuO	Fe_3O_4
Fe_3O_4	-	-	-	-	-	8.36	-	-	45
CuO	-	-	4.69	3.42	5.14	-	-	15	-
ZnO	3.25	5.21	-	-	-	-	20	-	-
Fe_3O_4/CuO/ZnO	3.24	5.21	4.69	3.42	5.13	8.37	23	15	38
Fe_3O_4/CuO/3ZnO	3.25	5.21	4.69	3.45	5.13	8.37	25	15	36
Fe_3O_4/CuO/5ZnO	3.25	5.21	4.68	3.45	5.13	8.35	26	15	35

Table 2. Band Gap. Magnetization, and BET analysis of pure Fe_3O_4, CuO, ZnO nanoparticles and Fe_3O_4/CuO/ZnO nanocomposites with different molar ratio.

Sampel	Band Gap (eV)	Magnetization (emu/g)	Surface Area(m^2/g)	Pore Diameter (cc/g)	Meseporous Volume (nm)
Fe_3O_4	-	82	-	-	-
CuO	1.54	-	-	-	-
ZnO	3.37	-	-	-	-
Fe_3O_4/CuO/ZnO	2.83	46	11.99	1.2	0.06
Fe_3O_4/CuO/3ZnO	3.06	23	37.09	2.99	0.13
Fe_3O_4/CuO/5ZnO	3.16	17	39.36	3.17	0.11

The XRD patterns of Fe_3O_4/CuO/ZnO nanocomposites, prepared Fe_3O_4, CuO, ZnO nanoparticles were given in Figure 1. As can be seen in Figure 1, the diffraction angles of $2\theta = 30°$, $2\theta = 30.14^o$, 35.49^o, 43.28^o, 53.76^o, 57.20^o, and 62.83^o correspond well with planes of cubic spinel phase of Fe_3O_4, while the diffraction angle of 32.39^o, 35.40^o, 38.62^o, 48.65^o, 53.3^o, 58.1^o, 61.44^o, 65.68^o, 66.17^o, 67.93^o, 72.30^o correspond with monoclinic phase of CuO and hexagonal wurtzites phase of ZnO detected at $2\theta = 32.12^o$, 34.48^o, 36.6^o, 47.76^o, 56.84^o, 63.02^o, 66.95^o, 68.23^o and 69.24^o. The absence of other mixtures of Fe_3O_4, CuO and ZnO diffraction peaks in the spectra confirms the formation of Fe_3O_4/CuO/ZnO nanocomposites. As shown in the figure, obviously, as the molar ratio of Fe_3O_4/CuO/ZnO nanocomposites increased from 1:1:1 to 1:1:5, the diffraction peaks of ZnO become prominent. The average crystallite size for pure nanoparticles and nanocomposites estimated using the well-known Debye–Scherer relation [16] and the values of the lattice parameters obtained using the Rietveld refinement were displayed in Table 1. The result shows that the lattice constant of all samples do not change significantly.

UV-Vis Diffuse reflectance spectroscopy is a powerful tool for obtaining information about the optical absorption properties and the band gap energies of materials.The band gap energies can be calculated from the diffuse reflectance spectra by performing a Kubelka–Munk analysis [17]. The values of the band gaps are tabulated in Table 2. As seen, all of the nanocomposites present a decreased band gap energy compared to that of the pure ZnO nanoparticles, but it is greater than that of the pure CuO nanoparticles.

Pore properties such as surface area, pore volume and size have a close relationship with the catalytic activity efficiency. The surface area the pore diameter are also shown in Table 2. It can be seen from the table that the nanocomposite with a higher ZnO component shows a larger specific BET surface area of approximately 39.36 m^2/g, which decreases as the ZnO content decreases.

Magnetic properties of Fe_3O_4/CuO/ZnO nanocomposites were measured using a vibrating sample magnetometer (VSM) at room temperature in the field range of 0 to 1 T. Table 2 shows magnetization data for all Fe_3O_4/CuO/ZnO nanocomposites with molar ratios of 1:1:1 to 1:1:5. The magnetization of pure Fe_3O_4 nanoparticles were also shown in the table. It is observed that the saturation magnetization in pure Fe_3O_4 nanoparticles (82 emu/g) is lower than that of the reported value (92 emu/g) [18]. These results may be understood on the basis of a core-shell model that predicts a spin canting at the surface of Fe_3O_4 nanoparticles. The saturation magnetization decreased further as CuO and ZnO nanoparticles were introduced into the nanocomposite system.

Figure 2 shows the ESR spectra recorded at room temperature for Fe_3O_4/CuO/ZnO nanocomposites with various molar ratios. The spectra show broad resonance peaks that can be considered as a superposition of several overlapping signals that are too close to be separated with confidence.Therefore, we have carefully studied the spectra and found that the line position, the line width and the line intensity of all signals vary with the molar ratio. The ESR spectra can be fitted satisfactorily to four overlapping signals at (i) a g value range from 2.6591 to 2.5000, (ii) a relatively constant g of 4.4963 to 4.1382, (iii) a g value from and 2.0881 to 2.0194 and (iv) a g value from 1.9976 to 1.9701, indicating the presence of Fe^{2+}, Fe^{3+}, Cu^{2+} [19] and native defects, such as doubly ionized oxygen vacancies, that can act as trapping states for electrons [20], respectively. ESR parameters, such as line width (ΔHpp), g values and integrated areas that reflect the total number of spins taking part in the resonance line, are given in Table 3. As seen from Table 3, with an increase in the molar ratio of Fe_3O_4/CuO/ZnO nanocomposites from 1:1:1 to 1:1:5, a decrease in the integrated areas of Fe^{2+}, Fe^{3+} and Cu^{2+} was observed, indicating that the total number of spins contributing to the ESR spectra decreased, while the integrated area of native defects increased.

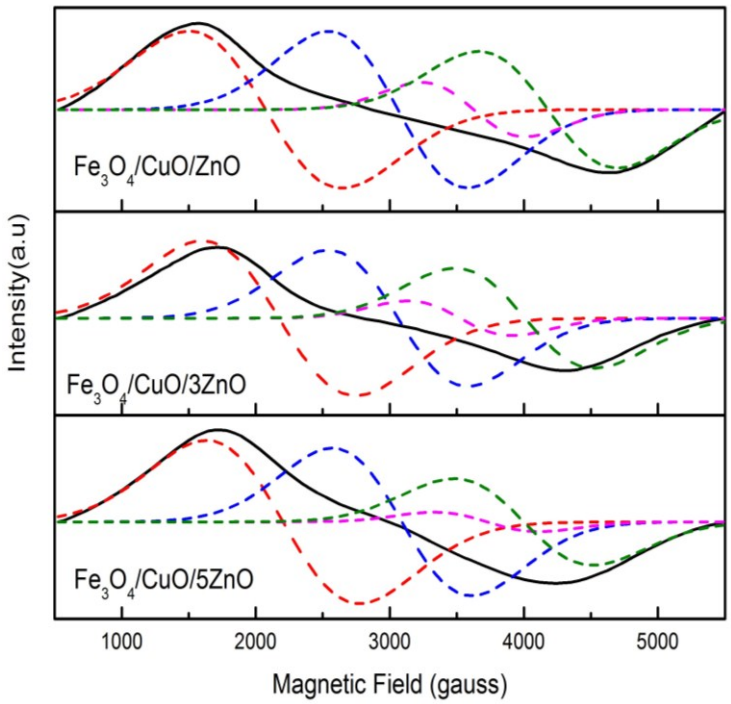

Figure 2. ESR Signal of nanocomposites Fe_3O_4/CuO/ZnO with different molar ratio.

Table 3. g value, Integrated Area, ΔHpp of ESR spectra of Fe_3O_4/CuO/ZnO nanocomposites with different molar ratio.

Sampel	g value	Integrated Area	ΔHpp	Signal Identification
Fe_3O_4/CuO/ZnO	4.4963	9.33 x 10^8	1141.993	Fe^{3+}
	2.6591	7.72 x 10^8	1039.195	Fe^{2+}
	2.0881	1.51 x 10^8	624.8679	Cu^{2+}
	1.9701	4.87 x 10^8	1076.574	Oxygen vacancy
Fe_3O_4/CuO/3ZnO	4.2157	9.04 x 10^8	1201.266	Fe^{3+}
	2.6514	6.41 x 10^8	1039.341	Fe^{2+}
	2.0254	5.34 x 10^8	577.8902	Cu^{2+}
	1.9408	4.92 x 10^8	1034.846	Oxygen vacancy
Fe_3O_4/CuO/5ZnO	4.1382	9.20 x 10^8	1221.993	Fe^{3+}
	2.5015	4.99 x 10^8	919.858	Fe^{2+}
	2.0194	3.30 x 10^8	559.858	Cu^{2+}
	1.9976	5.08 x 10^8	996.574	Oxygen vacancy

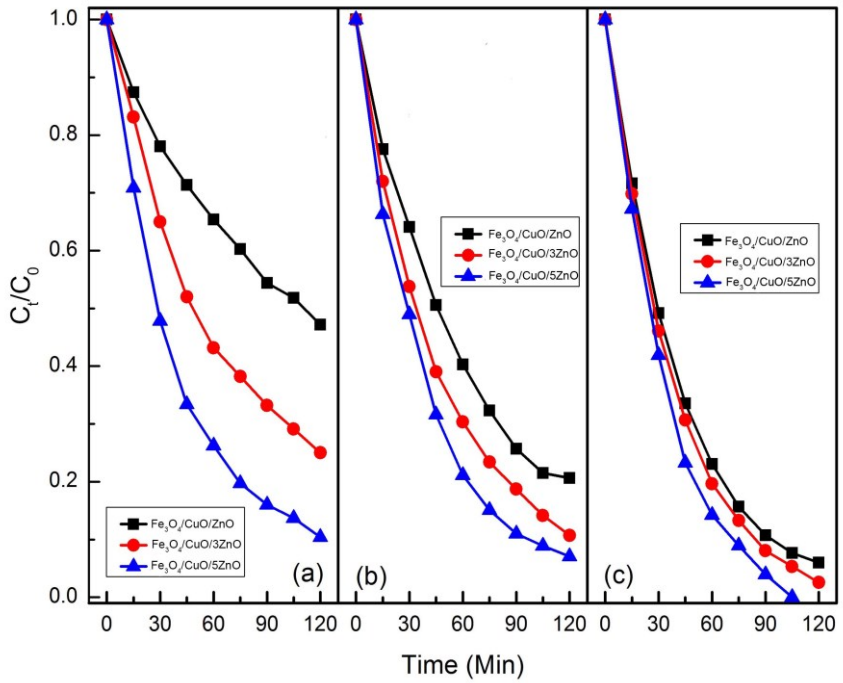

Figure 3. (a) Photocatalytic, (b) sonocatalytic, and (c) Sonophotocatalytic performance of Fe_3O_4/CuO/ZnO nanocomposites with different molar ratio.

The degradation of MB in aqueous solution was investigated in the presence of Fe_3O_4/CuO/ZnO nanocomposites under irradiation of ultrasonic (US) and UV light individually as well as in combination (US+UV). Figure 3 shows under ultrasonic, UV light and combination of both irradiation sources, the degradation of MB conducted at pH values of 13 in the presence of Fe_3O_4/CuO/ZnO

nanocomposites. In this study, the initial concentration of MB and the concentrations of nanocomposites as catalysts were fixed at 20 mg/L and 0.3 g/L for all the degradation processes, respectively. As can be seen from the figure 3, Fe_3O_4/CuO/ZnO nanocomposites with molar ratios of 1:1:1, 1:1:3 and 1:1:5 were able to degrade approximately 53%, 75%, 90%, 79%, 89%, 93% and 94%, 97%, 100% of MB, for UV, US and US+UV, respectively, within 2 h. It is clear that Fe_3O_4/CuO/ZnO nanocomposites with molar ratios of 1:1:5 shows the best catalytic performance under all irradiation sources. The degradation is more facile in sonocatalysis compared to photocatalysis. The degradation of 100% was achieved in the presence of UV + US within less than 2h, suggesting the synergy interaction in appropriate manner between UV light and US irradiation plays an important role in enhancing the catalytic activity.

It is known that reusability and stability of catalysts are important parameters of the degradation process and are important issues for practical applications. In this experiment, Fe_3O_4/CuO/ZnO nanocomposites could be easily recovered from the solution using a permanent bar magnet. To evaluate the stability of the catalyst under UV, US and UV+US irradiation, the Fe_3O_4/CuO/ZnO nanocomposites with a molar ratio of 1:1:5 were repeatedly used for four cycles. The stability was evaluated by reusing the catalyst with the same quantity of fresh MB after each run. The results are shown in Figure 4. After four cycles, degradation efficiencies of 75%, 87% and 93% were obtained for UV, US and UV+US, respectively. These results indicated that Fe_3O_4/CuO/ZnO nanocomposites were fairly stable under the condition used in this study.

To understand the active species involved during the degradation of MB in the presence of Fe_3O_4/CuO/ZnO nanocomposites with molar ratio 1:1:5, free radical trapping experiments were carried out by adding various scavengers. Tert-butyl alcohol was used to scavenge hydroxyl radicals, while ammonium oxalate and $Na_2S_2O_8$ were used to scavenge generated holes and electrons, respectively. As shown in Figure 5 after adding scavengers the degradation efficiency of MB exhibited a gradual decrease and a noticeable inhibition was observed in the presence of ammonium oxalate, suggesting the important role of hole in the degradation process of MB. From Figure 5 it is seen that holes were the primary active species in degradation of MB for UV, US and UV+US.

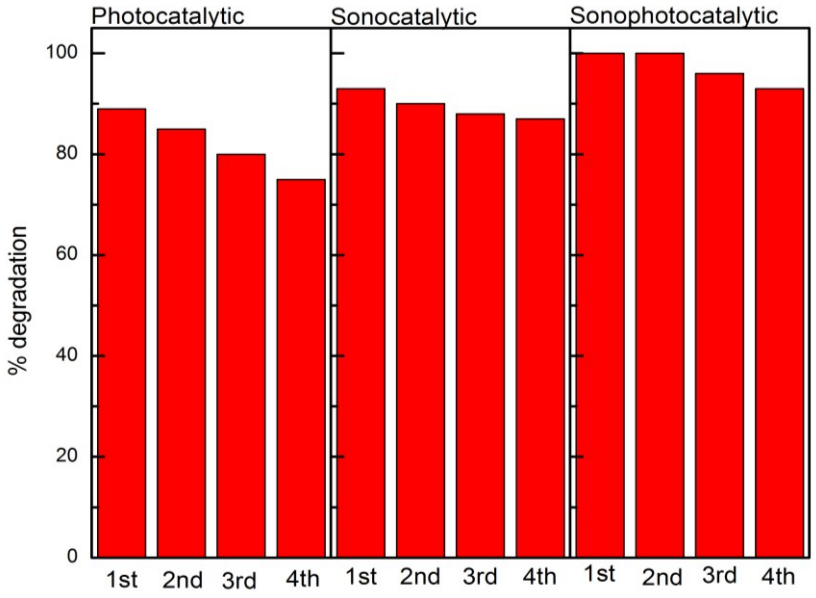

Figure 4. Reusability of Photocatalytic, sonocatalytic, and Sonophotocatalytic. Performance Fe_3O_4/CuO/5ZnO nanocomposites.

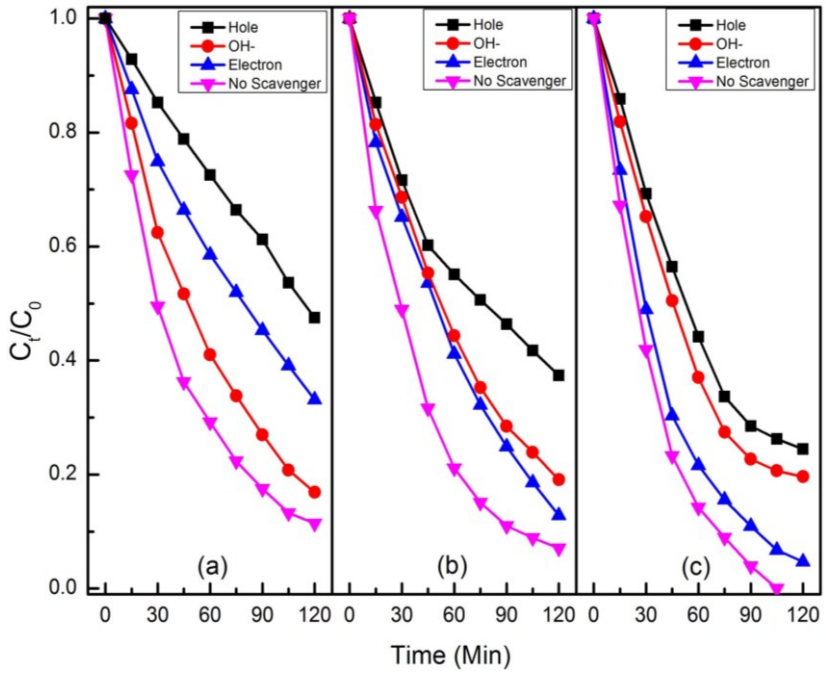

Figure 5. Effect of scavenger on (a) Photocatalytic, (b) sonocatalytic, and (c) Sonophotocatalytic. Performance of Fe_3O_4/CuO/ZnO nanocomposites with molar ratio 1:1:5.

Photocatalytic degradation of methylene blue in aqueous solution by UV irradiation has been reported in our previous papers [8]. However, a mechanism of UV+US processes in the presence of ternary nanocomposites has not been issued yet. The results of this study showed clearly that the oxidation process of methylene blue in all processes was holes dependent. Therefore, the presence of Fe_3O_4/CuO/ZnO nanocomposites should results in the formation of holes in the irradiation solutions. From the diffuse reflectance spectroscopy measurements, the band gap energies of CuO and ZnO were 1.54 and 3.37eV, respectively. The band structure of the above individual components seems unfavorable for the separation of photo- or sonogenerated electrons and holes. However, in the Fe_3O_4/CuO/ZnO nanocomposites, a sufficient contact between the components is a crucial factor in forming effective separation and transfer of electrons and holes. A heterojunction and a new energy band structure will be formed after all components are contacted and may change the charge transfer process. As Fe_3O_4/CuO/ZnO nanocomposites is irradiated by UV light, the ZnO can be activated due to its wide band gap energy [21]. Therefore, it can be seen that the nanocomposites with a molar ratio of 1:1:5 exhibit better photocatalytic performance in the UV.

The degradation of MB is more facile in the US compared to UV. The MB can be rapidly degraded in the presence of Fe_3O_4/CuO/ZnO nanocomposites with lower ZnO loading by US irradiation. It is known that the mechanism of sonocatalytic degradation is related to the acoustic cavitation [22-27]. Besides generating hot spot in the solution, sonoluminescence could also be involved, that excites Fe_3O_4/CuO/ZnO nanocomposites to act as a photocatalyst during sonication to form electron-hole pairs. These pairs can produce OH radicals ($OH^{\bullet}$) and superoxide anions ($O_2^{\bullet -}$) which can be decomposed MB. From scavenger technique, it is found that the degradation process of MB was holes dependent.

According to the predicted band energy position, under irradiation the generated electron in the conduction band of ZnO is prohibited from transferring to the conduction band of CuO by the energy barrier that exists at the interface between ZnO and CuO [21-22]. However, the generated holes in the valence band of ZnO will be readily transferred to the valence band of CuO. The electron could also be

transferred to electron trapping states, such as doubly ionized oxygen vacancies formed in the Fe_3O_4/CuO/ZnO nanocomposites. In this process, the electron collected in the trapping state can later react with absorbed molecular oxygen to yield the superoxide radical, $O_2^{\bullet -}$. Simultaneously, the generated holes in the valence band can then react with the hydroxyl group (OH^-) to form a hydroxyl radical ($OH^\bullet$).

4. Conclusion

The purpose of this study was to investigate the degradation of MB under UV, US and UV+US irradiation. The results showed that MB can be effectively removed bu using combination of UV and US irradiation. For individual operation of two modes of irradiation, US has more effeciency compared to UV. For all processes, the catalytic activity of Fe_3O_4/CuO/ZnO nanocomposites with molar ratio of 1:1:5 was the highest, probably due to its higher surface area.

References

[1] M. Ahmad, E. Ahmed, Z. L. Hong , W. Ahmed, A. Elhissi, N. R. Khalid, Ultrasound. Sonochem. 21 (2014) 761–773
[2] A. Houas, H. Lachheb, M. Ksibi, E. Elaloui, C. Guillard, J. M. Herrmann, Appl Catal B: Environ. 31 (2001) 145–157.
[3] M. Saquib, M. Muneer, Desalination 155 (2003) 255–263.
[4] V. Meshko, L. Markovska, M. Mincheva, A.E. Rodrigues, Water Res. 35 (2001) 3357–3366.
[5] W. S. Kuo, P.H. Ho, Chemosphere 45 (2001) 77–83.
[6] J. K. Im, J. Yoon, N. Her, J. Han, K. D. Zoh, Y. Yoon. Sep. Purif. Technol. 141 (2015) 1–9
[7] P. Chowdhury, T. Viraraghavan, Sci. Total. Environ. 407 (2009) 2474–2492.
[8] A. Taufik, I. K. Susanto, R. Saleh. Mater. Sci. Forum. 827 (2015) 37-42
[9] N. Talebian, M. R. Nilforoushan, F. J. Mogaddas, Chem. Eng. J. 39 (2013) 4913-4921
[10] S. Matzusawa, J. Tanaka, S. Sato, T. Ibusuki, J. Photoch. Photobio A. 149 (2002) 183–189.
[11] Y. Kado, M. Atobe, T. Nonaka, Ultrasound. Sonechem. 8 (2001) 69-74.
[12] E. Selli, J. Phys. Chem. 4 (2002) 6123–6128.
[13] L. Davydov, E.P. Reddy, P. France, P. G. Smirniotis, Appl Catal B: Environ. 32 (2001) 95–105.
[14] R. Saleh, N. F. Djaja, Spectrochim. Acta. B. 130 (2014) 581-590
[15] J. Hu, J. Ma, L. Wang, H. Huang, L. Ma, Powder Technol. 254 (2014) 556-562
[16] M. A. Ahmed, A. A. EL-Khawlani, J. Magn. Magn. Mater. 321 (2009) 1959‑1963
[17] B. Hapke, Theory of Reflectance and Emittance Spectroscopy, University Press, Cambridge, 1993.
[18] A. Jafari, S. F. Shayesteh, M. Salouti, K. Boustani, J Magn Magn Mater 379 (2015) 305–312
[19] A. V. Kucherov, D. E. Doronkin, A.Y. Stakheev, A. L. Kustov, M. Grill, J Mol Catal A-Chem 325 (2010) 73–78
[20] G. H. Mhlongo, D. E. Motaung, S. S. Nkosi, H.C. Swart, G. F. Malgas, K.T. Hillie, B.W. Mwakikunga, Appl Surf Sci 293 (2014) 62–70
[21] L. Sun, R. Shao, L. Tang, Z. Chen. J. Alloy Compd. 564 (2013) 55–62
[22] A. Roychowdhury, S. P. Pati, A. K. Mishra, S. Kumar, D. Das, J. Phys. Chem. Solids 74 (2013) 811-818.
[23] S. Thangavel, N. Raghavan, G. Kadarkarai, S.J. Kim, G.Venugopal. Ultrasound. Sonochem. 24 (2015) 123–131
[24] A. Khataee, A. Karimi, S. Arefi-Oskui, R. D. C. Soltani, Y. Hanifehpour, B. Soltani, S. W. Joo. Ultrasound. Sonochem. 22 (2015) 371-381
[25] K. P. Jyothi, S. Yesodharan, E. P. Yesodharan .Ultrasound. Sonochem. 21 (2014) 1787–1796

[26] N. Shimizu,C. Ogino, M. F. Dadjour, T. Murat. Ultrasound. Sonochem. 14 (2007) 184–190
[27] R. Saravanan, S. Karthikeyan, V. K. Gupta, G. Sekaran, V. Narayanan, Mater Sci Eng. ;.C 33 (2013) 91‑98.
[28] B. Li, Y. Wang, J. Alloy Compd. 47 (2010) 615‑623.